PROCEEDINGS, 13th Indonesia International GEOTHERMAL Convention & Exhibition 2013
Assembly Hall - Jakarta Convention Center Indonesia, June 12 – 14, 2013

LUMINESCENCE SPECTROSCOPY: A POWERFUL TOOL FOR STUDYING HYDROTHERMAL MINERALS. THE EXAMPLE OF REE-DOPED SILICA PHASES IN A SINTER DEPOSIT CLOSE TO LARDERELLO GEOTHERMAL FIELD, ITALY

A. Dallegno[1], G. Mazzoleni[1, 2], C. Pasqua[2]
1 Centro Studi Geominerari Luciano Holzner - Montemurlo (PO), Milan, Italy
2 ELC-Electroconsult, Baranzate (Milan - Italy)

e-mail: guido.mazzoleni@elc-electroconsult.com

ABSTRACT

A powerful and convenient methodology (cheap and easy to perform) has been successfully adopted for studying the mineralogy and the trace elements geochemistry of a silica-carbonate sinter deposit, linked to the Larderello geothermal field, Italy. The study carried out by means of luminescence spectroscopy added to microscope mineralogical analysis, proved to be useful as a complementary tool to investigate geothermal systems, both fossil and active, providing indications about the physical-chemical characteristics of the reservoir. The case-study site is located at La Sassa (Pisa Province, Tuscany). The area shows: (*i*) 'classical' hydrothermal mineral deposits along a network of fractures, and (*ii*) three Carlin-type gold mineralizations described in Italian ore deposit geology literature (La Sassa, Frassine and Campigliola). Minerals which formed in hydrothermal systems are commonly doped with 'foreign' trace-elements, as a replacement for 'base-component' elements in their crystalline lattice. Such a replacement, and lattice defects due to particular growth mechanisms in hydrothermal environment, often make involved minerals capable to fluoresce under ultraviolet light. A calibrated methodology, coupling adequate laser UV source and a high-resolution spectrometer, allows to determine the trace-elements content of hydrothermal minerals in the studied area and to establish the related environmental conditions. This analysis technique can be useful among the preliminary investigations, both on the outcrops and on boreholes cuttings. The studied silica-carbonate sinter deposit close to La Sassa formed where an ancient geyser was active. Silica mostly corresponds to (a) macro-crystalline α-quartz; (b) crypto- or micro-crystalline quartz (chalcedony); or rarely, (c) opal. The crystalline lattice of quartz includes 'foreign' elements like $(UO_2)^{2+}$, Tb^{3+}, Eu^{3+}, Dy^{3+}, and quantitatively subordinate Ce^{3+}, and Sm^{3+}, which activate a typical fluorescence, glowing different colors in the green-yellow to orange-yellow regions of the spectra, under different ultraviolet wavelengths.

La Sassa hydrothermal minerals show: (*i*) elements replacement in both silica phases and hosting calcite; (*ii*) lattice growth defects; (*iii*) enrichment in REEs, $(UO_2)^{2+}$, and polycyclic aromatic hydrocarbons (PAHs). These minerals are linked to early-stage evolution of the Larderello geothermal field. Similar mineral deposits are likely to be found in similar geological and geothermal contexts worldwide. Luminescence spectroscopy and UVF microscopy proved to be an expeditious tools in geothermal research, allowing to identify hydrothermal minerals and their fluid-metal sources parameters, linked to the various ore forming fluid processes. Combined with geochemistry, luminescence spectroscopy and UVF microscopy can identify trace elements, even when their content is below the threshold of sensitivity limits of the most common microprobe analyses.

KEY WORDS

Luminescence spectroscopy, UVF microscopy, Hydrothermal minerals, Fluorescent quartz, Silica-sinter, Larderello, Geothermal fields

LIST OF ACRONYMS AND ABBREVIATIONS

c-axis = vertically oriented axis of a crystal (usually the principal symmetry axis)
ICP-MS = inductively coupled plasma mass spectrometry
MPa = megapascal
NaCl eq. = salinity referred to equivalent per cent weight of sodium chloride
PAHs = polycyclic aromatic hydrocarbons
REEs = (rare earth elements, in this article acronym is specifically referred to the Lanthanide Series)
RMS = Root Mean Square
UV = ultraviolet light (electromagnetic radiation with a wavelength shorter than 400 nm)
UVF = fluorescence excited by exposure to ultraviolet light
λex = wavelength of excitation source

INTRODUCTION

First-step, general investigations in geothermal areas have to provide basic information about different topics, including geometry of the deep structures beneath the topographical surface, as a result of faulting and related fracture systems. Where an anomalous high geothermal gradient exists, this is commonly associated with the same geological structures affecting the sub-surface rock masses and allowing the circulation of fluids and the subsequent formation of hydrothermal minerals. The latter usually act as a trap for upward migrating chemical elements and ions, which can be remobilized from deep levels along deep-seated faults, especially when extension structures (graben, semi-graben, anular fault of caldera rims) are found. These elements and ions are easily remobilized toward shallower levels by hydrothermal fluids and obviously depend on the petrological/mineralogical characteristics of the buried rocks. The most common among these elements and ions are $(UO_2)^{2+}$, REEs, Hg, and others depending on local context. The same elements are commonly the goal of soil geochemistry prospection, and help in validating the indications provided by geophysics. Hydrothermal minerals reveal the presence of the mentioned elements, since the latter can commonly favor, or directly activate, the fluorescence of mineral species, which use to be inert when very pure in composition and lacking of substantial lattice defects. This is the case of quartz in its crystalline form (α-quartz), which is described as non-fluorescent in almost any mineralogical database. The locality described in this article is one of the very few in the world which yields fluorescent quartz and the only one which has been studied in detail (Dallegno and Mazzoleni, 2012).

GEOLOGICAL SETTING

The geology of Larderello geothermal field, framed in the regional setting of Tuscan Apennine, is thoroughly described in several articles (Benvenuti *et al*., 2004; Bertini *et al*., 2006; Cavarretta and Puxeddu, 1990; Conticelli, 2004; Dini *et al*., 2005; Gianelli and Ruggieri, 2000). Epithermal gold mineralizations are i.e. described in Lattanzi (1999), besides several Italian-written articles, University's Thesis and internal reports.

It is possible to summarize the following basic features: La Sassa locality lies in Southern Tuscany, close to the Tyrrhenian Sea (a triangular area with active oceanic crust formation and Plio-Quaternary granitic intrusions ascent to very shallow depth). The regional setting shows crustal thinning and mantle upwelling, giving rise to extension tectonics, widespread presence of igneous rocks (Tuscan Magmatic Province), both intrusive and effusive, accompanied with an anomalous high geothermal gradient and scattered ore deposits. La Sassa hamlet (Montecatini Val di Cécina municipality) is located along one of the main extensional faults, trending roughly NW-SE, giving rise to horst-graben styled Neogene basins. The site is also at the western edge of Larderello Geothermal field. Main regional features are resumed in Figure 1 and the detail about La Sassa local geology is shown in Figure 2.

Close to La Sassa hamlet, a rock body made of silica crops out. The body, previously described as 'vein-like deposit', is a partly eroded, huge primary silica sinter deposit, which had been truncated by a set of 130-170° N trending normal faults (Dallegno and Mazzoleni, 2012). The rock body consists of several alternating quartz-chalcedony bands. Eggshell textures and cavities coated with crusts of quartz and chalcedony, typical of mature silica sinter deposits, are partly preserved (Figure 3).

Adjacent to the sinter deposit, remnants with typical hot springs characteristics occur, such as orbicular, textured, recrystallized quartz, probably related to earlier 'geyser eggs'. The silica sinter is partly covered by a younger carbonate-siliceous sinter. Hence, the latest emissions occurred in a lower temperature environment favorable to carbonate deposition, up to travertine-like terms. In this late-stage sinter, semi-translucent white concentric bands of radiating quartz are found. They may be 'geyser eggs' torn away from the original *substratum* and redeposited within a late-stage travertine incrustation. Where brecciated and strongly silicified zones replaced the sinter, one may find remarkable specimens of white, fine grained, textured, microcrystalline quartz. This quartz represents the final stage of silica-gel deposition (during the medium-grade thermal episode), which sealed some feeding conduits of the hot spring; it is usually non-fluorescent, but within its mass, some rare twisted remnants may glow a faded orange-yellow (Figure 4). Peripheral zones, lateral to the original vents of the hot fluids, are strongly silicified; and rocks had been transformed into jasperoids (which are almost non-fluorescent).

MINERALOGY

Due to its particular and almost unique mineralogy (quartz in crystalline form which fluoresces a brilliant lemon-yellow under any ultraviolet wavelength, Figure 5), this locality was noted by collectors in the early-1970s and a sample was sent to the British Museum in 1972, to be analyzed. Such a fluorescence is not due to fluorescent inclusions (like hydrocarbons in Herkimer-type autigenic quartz) and resists to both mechanical shock and heating. The sample was ground into very fine dust and the finest particle powder fluoresced. In 2012, authors sent

other samples to be tested in a muffle kiln for ceramic materials in Milan's Bicocca Earth Sciences department, reaching 1000 °C, and temperature did not destroy the luminescence (Dr. Paolo Gentile, personal communication).

In the study area, silica is found as: (a) macro-crystalline α-quartz; (b) crypto- or micro-crystalline quartz (chalcedony); or rarely, (c) opal. Fluorescing silica occurs as spheroid aggregates of radiating quartz, consisting of densely packed glassy crystals. These nodule-like aggregates are scattered along tectonic trends (post-Mio-Pliocene), usually in a non-fluorescent matrix of carbonates (calcite, minor dolomite, scarce ankerite) and quartz varieties (pale microcrystalline quartz, multi-colored chalcedony).

Some specimens are fragments of spheroid aggregates generally formed by several nodules with individual crystallized centers that have grown together, developed radiating fibers up to 6 cm in length, and show a sharply zoned pattern of concentric bands (colorless translucent, pale honey yellow, and darker brownish yellow) under white light. Fluorescence color changes from band to band, depending on the white light color (Figure 6).

Polynucleate spheroid aggregates with radiating fibers consist of low α-quartz and may measure more than 10 cm across. The crystallized nucleus in the center of the concentric growth banding may correspond to one (or more) prismatic tabular crystals of baryte, a small cavity, or a sub-millimeter crystal of quartz. Under the microscope, in polarized light, the radiating quartz shows a structure typical of quartzine-length-slow: the quartz fibers are stacked along the *c*-axis [0001].

Usually, this length-slow silica phase is replaced by second generation neogenic non-fluorescent quartz, with a sharp euhedral *habitus* oriented differently than the former fibers (Figure 7). Such non-fluorescent quartz is often associated with a late-stage vein filling and inter-granular formation of sulphides and oxides / hydroxides (pyrite, marcasite, arsenopyrite, hematite, magnetite, lepidocrocite, goethite, stibnite, sphalerite), baryte, and rare secondary arsenates (scorodite).

In the brightest fluorescing zones of the radiating quartz, the second-generation euhedral quartz is completely lacking, as inclusions, although it may be found as a late stage filling of cavities (Figure 8). The fibers, observed microscopically under crossed Nicols, show a positive lengthening. Based on field evidence and laboratory tests, the length-slow radiating fibrous quartz is considered as typical of an environment with temperatures higher than 150 °C and high concentration of electrolytes (NaCl, KCl, etc.) in water solutions. This structure of quartz is usually found in neutral-alkaline sedimentary and hydrothermal environments (Folk and Pittman, 1971).

An uneven cleavage along *{1011}* or *{0111}*, suggests that quartz underwent some degree of deformation, not exceeding 4 Kbar pressure or 450 °C temperature (Deer *et al.*, 1966; Bloss and Gibbs, 1963; Flörke *et al.*, 1981). Minute fragments of tourmaline crystals included within the quartz fibers are generally oriented parallel to the fibers' long axis. According to its optical characteristics, this tourmaline should belong to the dravite-ferridravite series. Cavarretta and Puxeddu (1990) studied samples from 4 km deep drillings in the Larderello geothermal field and recognized an early stage of hydrothermal metamorphism, characterized by a paragenesis of abundant dravite-ferridravite series tourmaline, accompanied by biotite, a Ca-rich member of plagioclase, K-feldspar, quartz and pyrrhotite. They defined the environmental conditions as: lithostatic pressures of 0.75-1.0 Kbar, temperatures from 400-600 °C, and a high concentration of NaCl eq. (50-60% in wt.).

In La Sassa study area, where the extensional Apennine faults (~130° N) intersect the older compressive faults (~170° N), especially in points most affected by brittle tectonics, surface field evidence (hydrothermal deposits) indicates that fracturing reached crustal levels so deep that it may have created the early-stage escape zones for magmatic fluids (high concentrations of NaCl, silica phases, REEs, B, F, Li, and Al). This is the depositional environment of the glowing quartz. In carbonate-gangue veins, where the radiating nodules of the yellow fluorescing quartz and their fragments have been found; silicification zones of carbonate gangue enclosing clasts of densely grained microcrystalline quartz with fading edges also appear. The clasts are sometime white to pale grey-yellow, but are more frequently a darker yellow-brown, probably due to enrichment with polycyclic aromatic hydrocarbons (PAHs).

The fluorescent quartz, in any of its forms, is genetically linked to an early-stage hydrothermal metamorphism in the Larderello geothermal field. The greater portion of the carbonate gangue corresponds to subsequent, late-stage episodes of low temperature hydrothermal reactivation. Based on isotopic geochemistry data and micro-thermometric study of fluid inclusions in the different carbonate mineral phases of vein filling in the La Sassa area, Gianelli *et al.* (1997) and Bertini *et al.* (2006) defined the following:

- The deposition temperature as ≤ 150 °C;
- The apparent salinity (1.8-2.1 wt.% NaCl eq.);
- The geochronological age of calcite between 7,000-100,000 years (^{230}Th / ^{234}U dating on some samples).

LUMINESCENCE SPECTROSCOPY

The main goal of this paper is to show the methodology which has been used in order to define the various activators involved in the fluorescence of La Sassa quartz. Such a fluorescence is found in four main kinds of quartz:

1. translucent, colorless to whitish, fibrous-radiating (Figure 6);
2. pale yellow, fibrous-radiating to euhedral (Figure 5);
3. pale honey-yellow artichoke-type crystals, a rare split-growth due to important lattice defects (Figure 9);
4. white to pale gray saccharoid-textured (Figure 11).

Each kind is characterized by four different trends in excitation spectra curves (Drawings 1, 2, 3 and 4). All excitation spectra were obtained by means of steady-state spectroscopy, using a high resolution Kvant (Spectra SN 3K9880 model) spectrometer with an optical resolution ranging between 0.5-2 nm, signal noise ratio 250:1, dark noise < 10 RMS counts, and a 300 or 500 mW diode laser with λex = about 405 nm as a violet source. All excitation spectra have been obtained by following the methodology described in Dallegno and Mazzoleni (2012).

A high optical resolution instrument (0.5 nm) allowed to separate and determine some well defined peaks (Drawing 1). The following chemical elements and ions are suspected to be the activators of La Sassa minerals:

- $(UO_2)^{2+}$, Tb^{3+}, Eu^{3+}, Dy^{3+}, Sm^{3+}, Ce^{3+} for the quartz;
- Sm^{3+}, Dy^{3+}, Eu^{3+}, Mn^{2+} for the midrange UV red-fluorescing accompanying calcite (Figure 10).

It is strongly suspected that the presence of polycyclic aromatic hydrocarbons (PAHs), as impurities, can produce peaks in the visible part of the spectrum. Such PAHs impurities are normally found in hot spring systems bearing precious metal mineralization, and can also form mineral species like idrialite (curtisite) and pendletonite.

Drawing 5 shows the overlapping of two spectral curves obtained from two different quartz samples. The first curve (green line) is from a fibrous-radiating quartz found in the siliceous sinter; the second curve (red line) is from a saccharoid-textured quartz sample found along the same tectonic structure as a source, but at a roughly 60 m lower topographical elevation (corresponding to a deeper level in the sinter deposit). The fluorescence of latter sample is clearly shifted toward the red region of the spectrum, compared with the fluorescence of the sample collected at a more surficial point. Such difference depends on less luminescence centers due to $(UO_2)^{2+}$ and more centers due to $Dy^{3+}$and Sm^{3+}.

In Drawing 6, the spectral curves of Drawing 5 are compared with a third curve (black line) corresponding to the excitation of quartz in artichoke-type crystals. It is clearly shown that the spectral curve of latter type of quartz represents the 'merging' of the other two curves (green and red lines). This demonstrate that artichoke-type crystals are effective traps for several activators of luminescence. Morevover, the kind of crystal growth (fibrous-radiating, saccharoid-textured, artichoke-type) appears to be selective in allowing the incorporation of the different activators in the quartz lattice. Results from our investigations agree with the most recent literature; in particular, the studies of several quartz samples from silica sinter deposits associated with epithermal gold mineralization in different localities in the world, which have been analyzed by ICP-MS for trace elements determination. They demonstrated that REEs, U, Th, Be, Te, Cs, Rb, Y etc., as incompatible trace elements, can actually be present in some hydrothermal silica samples (Tonguç *et al*., 2011; Smith *et al*., 2011). These experimental evidences confirm how particular and extreme, in terms of chemical-physical characteristics, the hot spring environment can be, so that quartz often undergoes a 'flash crystallization' (i.e. forming 'artichoke' crystals, or densely packed radiating crystals). Actually, at La Sassa it is evident that these particular crystallization kinds of quartz is the chemical-physical clue which allows the entering of seemingly incompatible trace elements.

Various authors presented some models of REEs patterns contained within silica sinter quartz, pointing out that such patterns could even allow to identify the locality the samples originate (Tonguç *et al*., 2010 and 2011). This hypothesis of different REEs patterns, distinguished by the siliceous sinters outcrops, is in close agreement with the authors' interpretation of the La Sassa silica sinter deposit. It indicates the possibility of an original and unique association of some chemical elements and compounds (REEs, U, PAHs) responsible for direct activation or co-activation of La Sassa quartz fluorescence.

DISCUSSION

We believe that the carbonate-hosted fluorescing quartz from La Sassa is genetically linked to an early-stage of hydrothermal metamorphism of the Larderello geothermal field, where the La Sassa vein system is a component of its peripheral zone. According to Gianelli and Ruggieri (2000); Ruggieri *et al*. (2011), this early-stage contact metamorphism is characterized by magmatic fluids with high concentrations of electrolytes (NaCl, KCl) and silica

gel, with temperature in the range of about 500-700 °C and pressure of about 100-140 MPa. These original fluids are effective in transporting elements (like REEs, B, F, Cl, Li, Al) and migrated upward to land surfaces, along extensional faults. Early-stage fluids with magmatic signature underwent a late-stage evolution, with phreatic water mixing, giving rise to a last hydrothermal phase with lower temperature and pressure (about 150-400 °C and 0-40 MPa).

A very important controlling factor is the suitability of the different crystalline lattices to trap 'foreign' elements and ions as luminescence activators. For instance, the sample in Figure 10 demonstrates that the sealing layer of calcite at to the contact with the fibrous-radiating quartz nodule is suitable for trapping Sm^{3+}, Dy^{3+} and Eu^{3+}. These luminescence activators, if contained within the original silica gel, may in part be migrated and trapped also within the calcite, only when the chemical-physical environmental conditions favored the fibrous-radiating crystal growth of the quartz, rather than the saccharoid-textured one. It is thus evident that part of calcite was coeval with the crystallization process of the original silica gel.

The siliceous sinter close to La Sassa is due to intense subaereal hot springs activity, which is spatially and genetically linked to low-grade Carlin-type gold mineralizations. Fluorescing quartz originates in outcrops located in the most tectonized area, with the strongest (hot spring) hydrothermal activity.

Several different generations of quartz, both fluorescing and non-fluorescing, have been described. Within the bright lemon yellow fluorescing quartz, the authors could individualize the presence of: (1) electrolytes and lithic fragments of tourmaline (dravite-ferridravite series) as solid inclusions within the radiating fibers of quartz; and, (2) a rare artichoke-type quartz which is typical of an environment where conditions forced a rapid growth of the crystalline aggregate, and has an abundance of trace elements like $(UO_2)^{2+}$, REEs, PAHs, Al, Na, B, Li, Zr, and F.

Based on preliminary indications using excitation laser spectroscopy, it is probable that the fluorescence of La Sassa quartz is due to the presence of $(UO_2)^{2+}$, Tb^{3+}, Eu^{3+}, Dy^{3+}, and quantitatively subordinate Ce^{3+}, and Sm^{3+} centers. Even at a few ppb, Ce^{3+} affects the fluorescence, since it transfers its excitation energy to Tb^{3+}, intensifying the green emission (maximum around 544 nm). Eu^{3+} and Dy^{3+} shift the fluorescence response toward the yellow-orange region of the spectrum, while the uneven presence of $(UO_2)^{2+}$ shifts the response towards the green region. Scattered PAHs and/or organic impurities may also contribute to La Sassa quartz fluorescence, mainly as co-activators: this role is demonstrated by the fact that the luminescence is not quenched, if the sample is heated at temperatures between 50 and 1000 °C.

All REEs have been found in their trivalent state enhancing luminescence efficiency; in addition, the original siliceous-melt co-activators, Al, B, Zr, and Li are present. This is probably due to a chemical-physical process of element selection, where REEs were converted to a trivalent state, probably due to local enrichments of metals like Fe, Zn, Pb, Cu, and Mo, located near buried magma. This change may have been completed while encountering widespread strata-bound metal ores (both massive and finely disseminated), commonly found in the Southern Tuscany crystalline basement during upwelling.

The convective cells of the hydrothermal system could have chemically interacted with evaporites and dolostones of Triassic sedimentary sequence, probably including beds yielding concentrations of organic compounds such as PAHs or mercaptans. These compounds, in a sol-gel hydrothermal environment, favored the introduction of activators like REEs in the early stage silica phases.

During the ascent of hydrothermal solutions toward shallower levels, mixing with meteoric water, boiling, and water-host rock interaction were intensified. In La Sassa, no significant deposits of alunite, kaolin or illite were observed; this suggests that the quantities of compounds like H_2S, HS^-, and SO_4^{2-} etc. in the hydrothermal fluids were quite low. This neutral to mildly alkaline ($pH \geq 7$) environment accelerated the coalescence and the precipitation of silica gel, which led to the development of a huge sinter deposit, later partly destroyed by extensional tectonics and erosion. The high concentrations of electrolytes, together with a temperature in excess of 150 °C, supported the fibrous radiating growth of the quartz. The last episode of low-temperature hydrothermal activity reworked and re-mobilized (also mechanically) the previously formed quartz, scattering it within a younger travertine-rich sinter and partly transforming it into a non-fluorescent neogenic quartz.

CONCLUSIONS

This paper highlights the potential of luminescence spectroscopy and UVF microscopy in geothermal research, as an expeditious tool which may contribute in distinguishing the various mineral phases (or generations of the same mineral) on the basis of different spectral characteristics of the luminescence. This can allow to determine the different hydrothermal phases and identify their fluid-metal sources parameters, linked to the various ore forming fluid processes during their chronological evolution. Moreover, when combined with geochemistry,

luminescence spectroscopy and UVF microscopy are a powerful tool for identifying, in the samples to be analyzed, some trace elements (and their spatial distribution within the sample mass), even when their content is minimal, below the threshold of sensitivity limits of the most common microprobe analyses.

ACKNOWLEDGEMENTS

Authors wish to thank *Centro Studi Geominerari Luciano Holzner* (a recently created research center for the preservation of the cultural heritage of mineralogy and ore deposit geology in Italian traditional mining areas) which supported the work by providing both the samples and the equipment in the mineralogical analysis laboratory, and ELC-Electroconsult S.p.A. Company, Milan, Italy, in addition to the following people: Matteo Boscardin, Renato Braga, Sergio Fantoni, Paolo Gentile, Maryann Manning, Roberto Nunziati, Paolo Pisani, Giovanni Pratesi, Karl Russ.

REFERENCES

Benvenuti, M., Boni, M. and Meinert, L. (2004), "Skarn deposits in Southern Tuscany and Elba Island (Central Italy)," In Guerrieri, L., Rischia, I. and Serva, L. (Eds.): Field Trip Guidebooks, 32nd International Congress, Florence 2004, *Memorie Descrittive della Carta Geologica d'Italia*, **63**, (2), APAT, Roma, 24 pages.

Bertini, G., Casini, M., Gianelli, G. and Pandeli, E. (2006), "Geological Structure of a long-living Geothermal System, Larderello, Italy," *Terra Nova*, **18**, 163-169.

Bloss, F.D. and Gibbs, G.V. (1963), "Cleavage in Quartz," *American Mineralogist*, **48**, 821-838.

Brogi, A. and Liotta, D. (2011), "Fluid Flow Paths in Fossil and Active Geothermal Fields: the Plio-Pleistocene Boccheggiano-Montieri and Larderello Areas," *Geological Field Trips SGI-ISPRA*, **3**, 2, 1-40.

Cavarretta, G. and Puxeddu, M. (1990), "Schoerl-Dravite-Ferridravite Tourmaline deposited by Hydrothermal Magmatic Fluids during the early Evolution of the Larderello Geothermal Field Italy," *Economic Geology*, **85**, 1236-1251.

Conticelli, S. (2004), "Pliocene-Quaternary Magmatism in Central Italy," In Guerrieri, L., Rischia, I. and Serva, L. (Eds.): Field Trip Guidebooks, 32nd International Congress, Florence 2004, *Memorie Descrittive della Carta Geologica d'Italia*, **63**, (4), 7-8 and 25-27.

Dallegno, A. and Mazzoleni, G. (2012), "A preliminary report: the glowing quartz from La Sassa, Tuscany, Italy," *Journal of Fluorescent Mineral Society*, **32**, 15-37.

Deer, W.A., Howie, R.A. and Zussman, J. (1966), "An Introduction to the Rock Forming Minerals," Longman Ed., Harlow, Essex, 528 pages.

Dini, A., Gianelli, G., Puxeddu, M. and Ruggieri, G. (2005), "Origin and Evolution of Pliocene-Pleistocene Granites from the Larderello Geothermal Field (Tuscan Magmatic Province, Italy)," *Lithos*, **81**, 1-31.

Flörke, O.W., Mielke, H.G., Weichert, J. and Kulke, H. (1981), "Quartz with Rhombohedral Cleavage from Magadascar," *American Mineralogist*, **66**, 596-600.

Folk, R.L. and Pittman, J.S. (1971), "Length-slow Chalcedony; a New Testament for Vanished Evaporites," *Journal of Sedimentary Petrology*, **41**, (4), 1045-1058.

Frondel, C. (1978), "Characters of Quartz Fibers," *American Mineralogist*, **63**, 17-27.

Gianelli, G., Puxeddu, M. and Ruggieri, G. (2001), "Contents of F, Cl, Li and B in the Granite Intrusions of Larderello, Italy," *Proceedings of 10th International Symposium Water Rock Interaction, WR-10, Villasimius (Italy)*, Vol. 2, 839-842.

Gianelli, G. and Ruggieri, G. (2000), "Contact Metamorphism in the Larderello Geothermal System," *Proceedings of World Geothermal Congress 2000, Kyushu-Tohoku, Japan*, 1163-1168.

Gianelli, G., Ruggieri, G. and Mussi, M. (1997), "Isotopic and fluid inclusion study of hydrothermal and metamorphic carbonates in the Larderello geothermal field and surrounding area, Italy," *Geothermics*, **26**, 393-417.

Götze, J., Plötze, M., Graupner, T., Hallbauer, D.K. and Bray, C.J. (2004), "Trace Element Incorporation into Quartz: a Combined Study by ICP-MS, Electron Spin Resonance, Cathodoluminescence, Capillary Ion Analysis and Gas Chromatography," *Geochimica et Cosmochimica Acta*, **68**, 3741-3759.

Lattanzi, P. (1999), "Epithermal precious metal deposits of Italy - an overview," *Mineralium Deposita*, **34**, 630-638.

Monecke, T., Bombach, G., Klemm, W., Kempe, U., Götze, J. and Wolf, D. (2000), "Determination of Trace Elements in the Quartz Reference Material UNS-SpS and in Natural Quartz Samples by

ICP-MS," *Geostandards and Geoanalytical Research*, **24**, (1), 73-81.

Perny, B., Eberhardt, P., Ramseyer, K., Mullis, J. and Pankrath, R. (1992), "Microdistribution of Al, Li and Na in α Quartz: Possible Causes and Correlation with Short-Lived Cathodoluminescence," *American Mineralogist*, **77**, 534-544.

Richter, D.K., Götte, T., Götze, J. and Neuser, R.D. (2004), "Progress in Application of Cathodoluminescence in Sedimentary Petrology," *Mineralogy and Petrology*, **79**, 127-166.

Ruggieri, G., Gianelli, G. and Giolito, C. (2011), "Fluid Evolution and Water-Rock Interaction in the Larderello Geothermal Field: Evidence from Mineralogical, Petrographic and Fluid Inclusions Studies," *Defining, exploring, imaging and assessing reservoirs for potential heat exchange*, Workshop 1, poster 16, Potsdam, Germany.

Smith, D.J., Jenkin, G.R.T., Petterson, M.G., Naden, J., Fielder, S., Toba, T. and Chenery, S.R.N. (2011), "Unusual Mixed Silica-Carbonate Deposits from Magmatic-Hydrothermal Hot Springs, Savo, Solomon Islands," *Journal of Geological Society*, **168**, 1297-1310.

Sunagawa, I., Iwasaki, H. and Iwasaki, F. (2009), "Growth and Morphology of Quartz Crystals: Natural and Synthetic," *Terra Scientific Publishing Company*, Tokyo, 202 pages.

Tonguç, U., Gasparon, M., Bolhar, R., Zhao, J.X., Feng, Y.X. and Jones, G. (2011), "Trace Element Composition of Near-Surface Silica Deposits - A Powerful Tool for Detecting Hydrothermal Mineral and Energy Resources," *Chemical Geology*, **280**, (1-2), 154-169.

Tonguç U., Gasparon, M. and Feng, Y.X. (2010), "Trace Element Composition of Near-Surface Silica Deposits as an Exploration Tool for Hot Dry Rock of Geothermal Systems," *Proceedings of World Geothermal Congress 2010, Bali, Indonesia*, (1-4), 25-29.

FIGURES

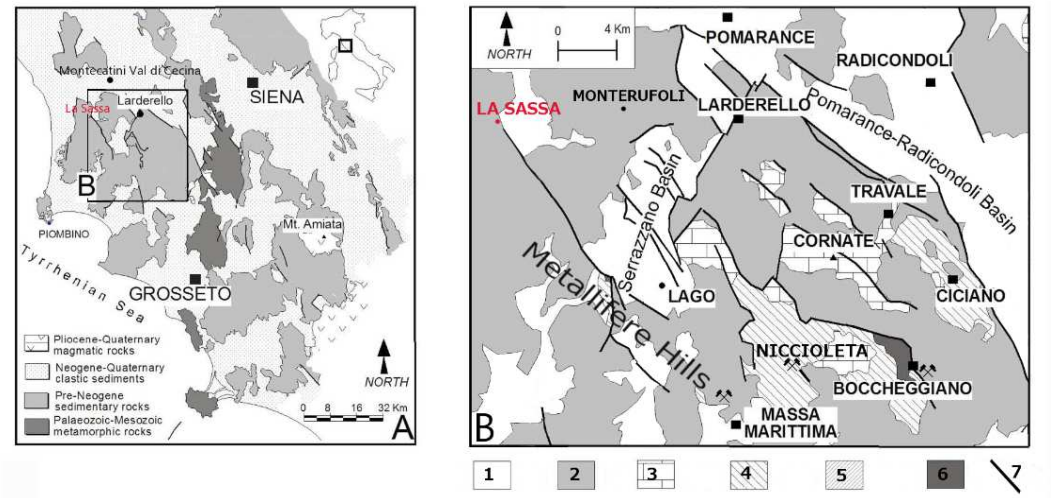

Figure 1: Geological sketch-map of Southern Tuscany (A); detail of Larderello Geothermal Field and Metallifere Hills ore deposits and mines (B). Re-drawn and modified after Brogi and Liotta (2011). Legend: (1) Neogene and Quaternary deposits, mostly as a filling of inter-montane basins; (2) Flysch-like Ligurian units, Eocene, with late Jurassic ophiolite slivers; (3) Late Triassic - early Miocene sedimentary sequence of Tuscan Nappe; (4) Late Triassic evaporites; (5) Quartz metaconglomerate, quartzite and phyllite of Triassic Verrucano Group; (6) Low-grade metamorphic Paleozoic crystalline basement, mostly phyllite; (7) Extensional faults.

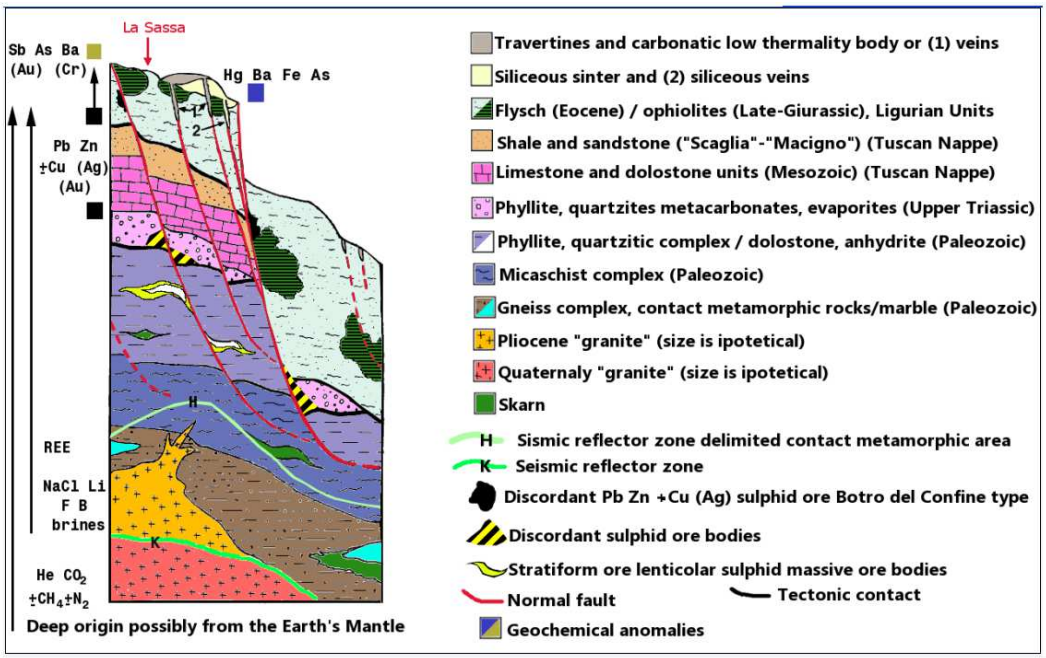

Figure 2: Tectono-stratigraphic sketch of geological units, geochemistry and ore deposits in the La Sassa area. This sketch is not to scale, nor does it strictly reflect the spatial relationships of the geological units. Deep structures after the interpretation of seismical reflection data in Larderello Geothermal Field by Bertini et al. (2006), Ruggieri et al. (2011). Geochemical data from Italian Ministry of Industry's unpublished internal reports; field data by the authors.



Figure 3: Detail of the sinter outcrop close to La Sassa, showing overlapping quartz-chalcedony bands with the typical 'eggshell' texture and voids due to preserved gas-filled cavities. Gray and rust-colored stains partly covering the rock are lichens. Photo Guido Mazzoleni.

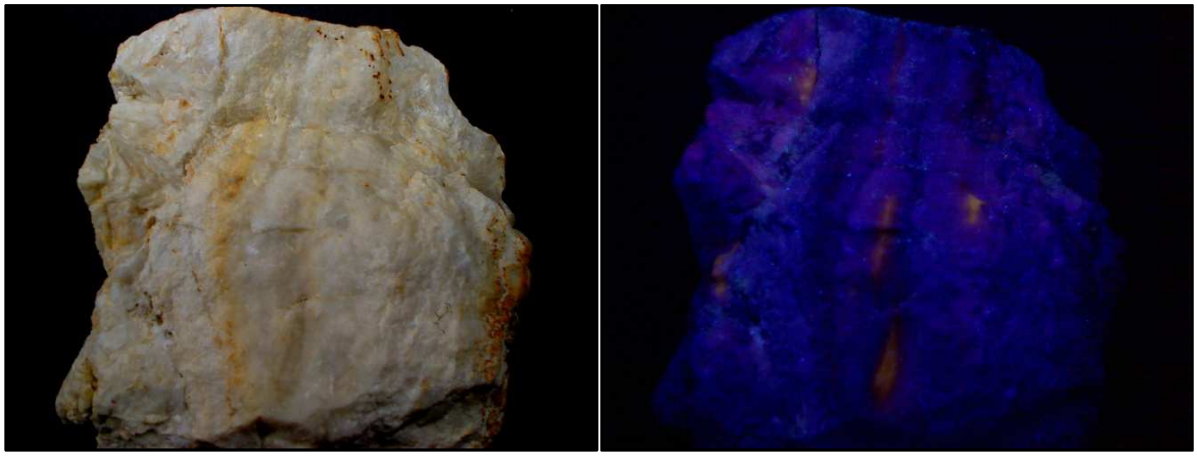

Figure 4: Remnants of fluorescent quartz within the non-fluorescent white, compact, saccharoid-textured quartz. The latter is a last-generation quartz which seals the hydrothermal vent. Sample CSG ls 41; Base of framed field about 25 cm. (left) white artificial light; (right) long-wave UV light. Photos Antonello Dallegno.



Figure 5: Fibrous quartz in radiating aggregates, in a partly etched carbonate matrix. Fiber's length up to 15 mm. (left) white artificial light; (right) short-wave UV. Sergio Fantoni collection, photos Roberto Appiani.

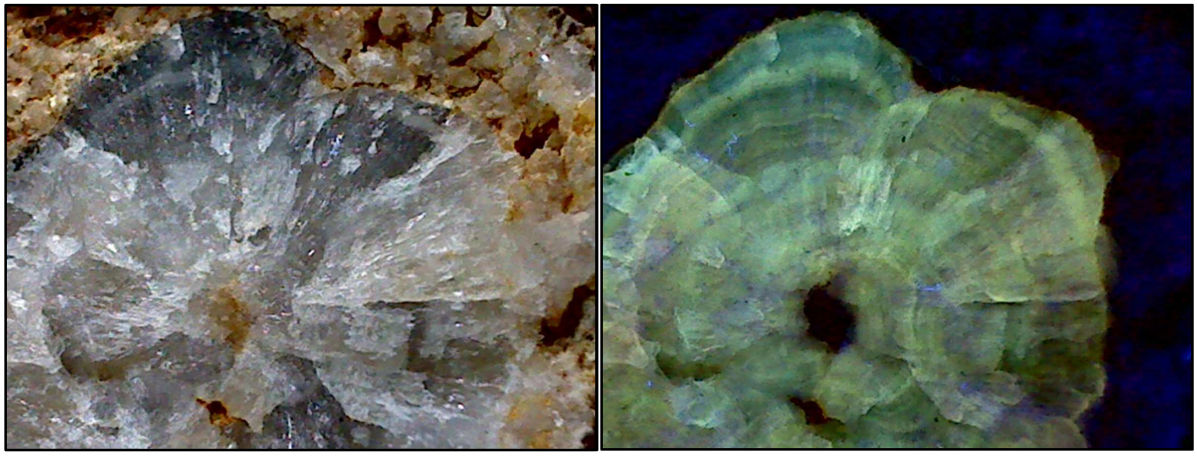

Figure 6: Concentric growth bands in colorless radiating quartz (sample CSG ls 7). Base of framed field about 80 mm. (left) white artificial light; (right) short-wave UV light. Photos Antonello Dallegno.

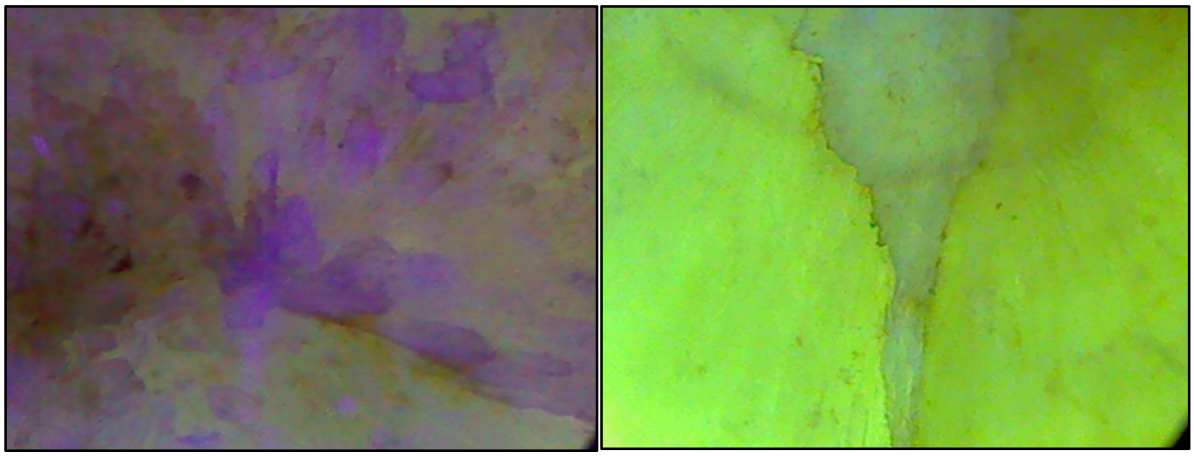

Figure 7 (left): Second generation quartz. Fluorescence microphotograph of thin section (sample CSG ls 4) under long-wave UV. Base of framed field 5 mm. Photo Antonello Dallegno.

Figure 8 (right): Suture zone between two fibrous radiating nuclei (aggregates) of fluorescent quartz. To be noted the absence of opaque minerals. Fluorescence microphotograph of polished section (sample CSG ls 8) under reflected long-wave UV. Base of framed field 5 mm. Photo Antonello Dallegno.

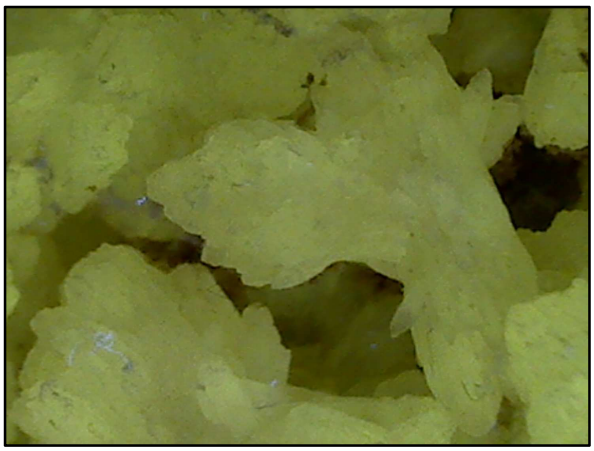

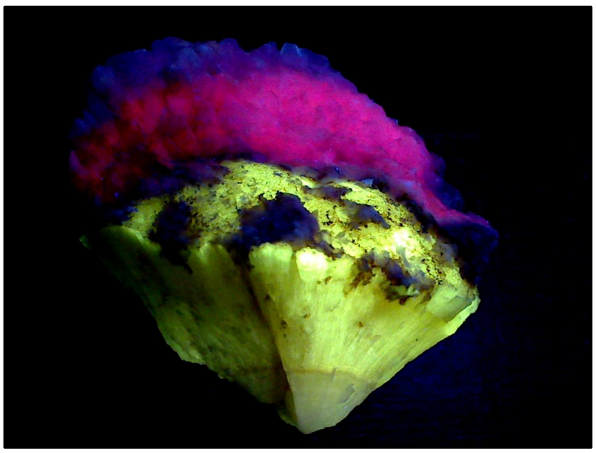

Figure 9 (left): *Artichoke-type quartz and non-fluorescing neogenic quartz crystals, under long-wave UV light. Small crystals grow from a unique common crystal center, in a clearly radiating fashion (sample CSG ls 8). Base of framed field 25 mm. Photo Antonello Dallegno.*

Figure 10 (right): *Red fluorescing calcite along the contact with lemon-yellow fluorescing fibrous radiating quartz, under midrange UV light. To be noted in the calcite, the sharp change between the outer rim of non-fluorescent and the thin fluorescent layer bordering the quartz aggregate. Sample from Renato Braga collection. Base of framed field 10 cm. Photo Antonello Dallegno.*

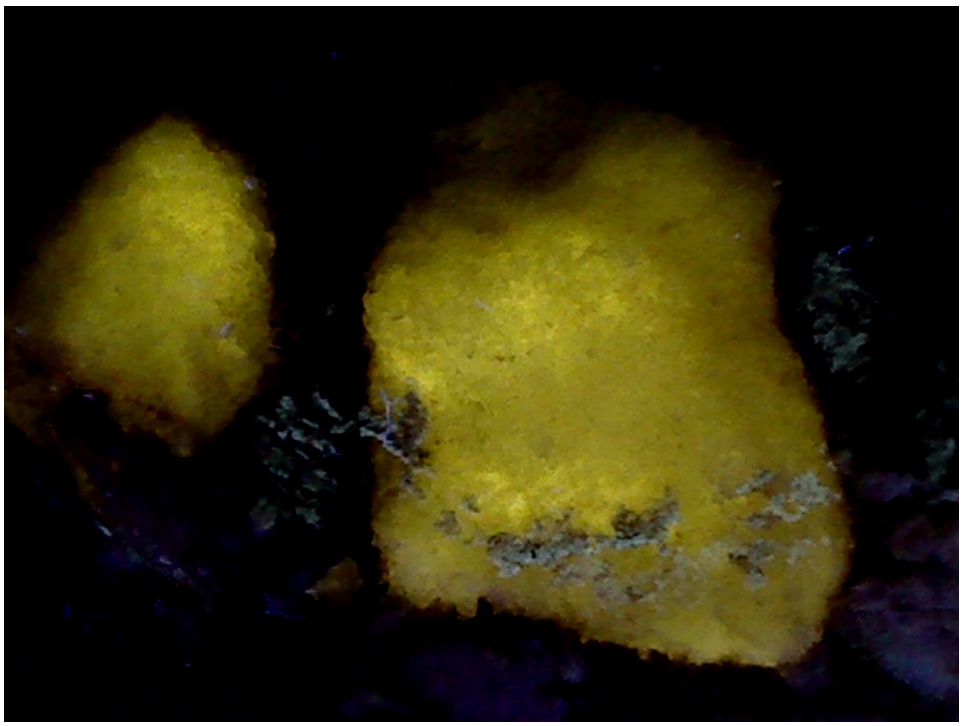

Figure 11: *White saccharoid-textured quartz (sample CSG ls 33), fluorescing orange-yellow under short-wave UV light. The calcite matrix associated with this crystallization kind of quartz is non-fluorescent since quartz trapped the whole amount of available activators. Base of framed field 5 cm. Photo Antonello Dallegno.*

DRAWINGS

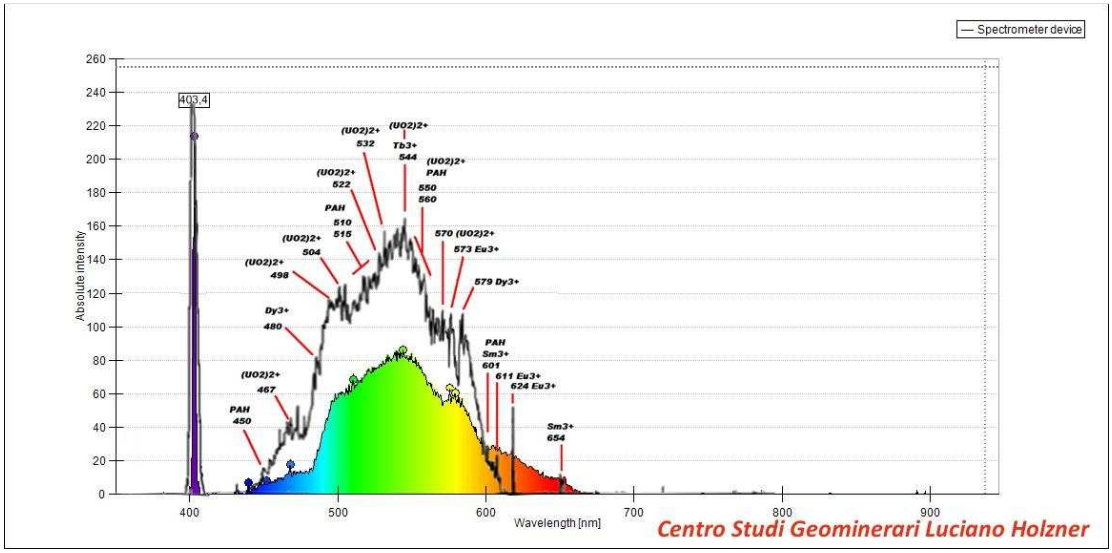

Drawing 1: Comparison by overlapping between two laser-induced steady-state luminescence spectra measured on the same point of a fibrous radiating pale honey yellow quartz (same sample from Renato Braga collection in Figure 10). Curve enclosing the colored area: λex = laser diode 405 nm 300 mW, use of optical fiber, optical resolution 2 nm. T = 300 K, - time 30 seconds. Black curve (above colored area): λex = laser diode 405 nm 500 mW, no use optical fiber, optical resolution 0,5 nm. T = 300 K, time 1 sec. The higher optical resolution (black curve) allows to better individualize the $(UO_2)^{2+}$, Tb^{3+}, Eu^{3+}, Dy^{3+}, Ce^{3+} and PAHs (or organic impurities) fluorescence centers. Spectra performed, processed and interpreted by Antonello Dallegno.

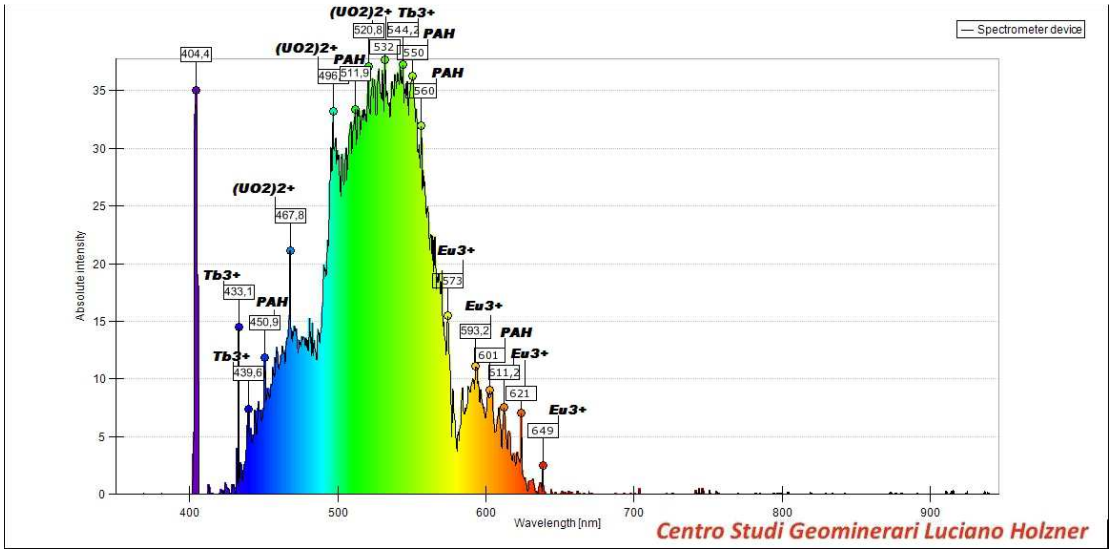

Drawing 2: Laser-induced steady-state luminescence spectrum of fibrous-radiating, white to very pale gray quartz showing $(UO_2)^{2+}$, Tb^{3+}, Eu^{3+} and PAH fluorescence centers. Note the clear extension towards green-blue regions of the spectrum, compared with the spectrum from saccharoid, white to very pale gray quartz (Drawing 4). This difference is due to a greater amount of $(UO_2)^{2+}$ and minimal amount of Dy^{3+} and Sm^{3+} fluorescence centers. λex = laser diode 405 nm 500 mW, optical resolution 0,5 nm, T = 300 K, time 1 second. Sample CSG ls 30. Spectra performed, processed and interpreted by Antonello Dallegno.

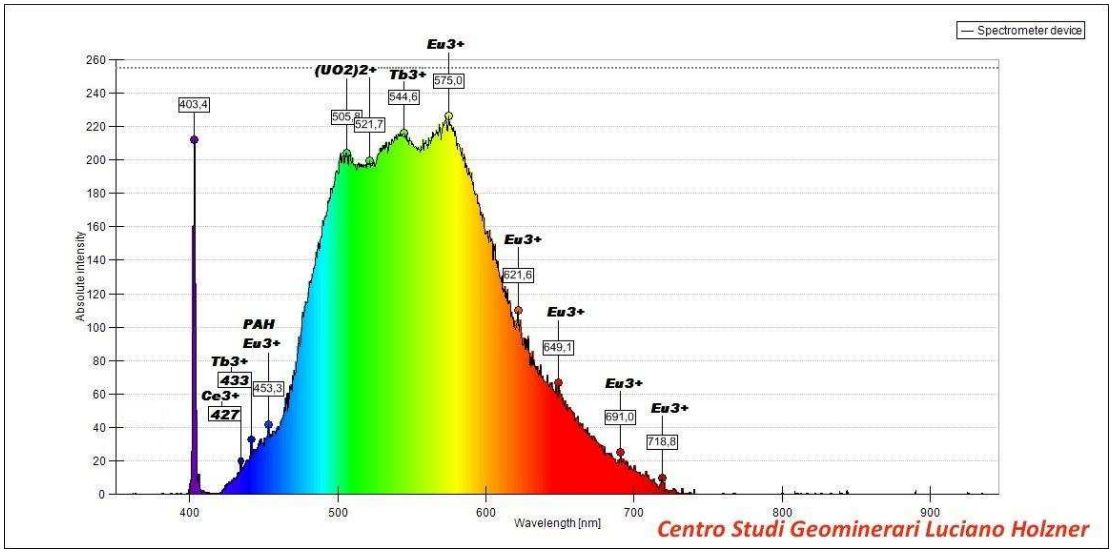

Drawing 3: Laser-induced steady-state luminescence spectrum of the euhedral artichoke-type pale honey yellow quartz crystal (sample CSG ls 8 in Figure 9), showing $(UO_2)^{2+}$, Tb^{3+}, Eu^{3+}, Ce^{3+} and PAHs (or organic impurities) fluorescence centers. This spectrum shows the exceptionally strong fluorescence of the artichoke-type crystals and the great increase of Eu^{3+} fluorescence centers. λex = laser diode 405 nm 300 mW, use of optical fiber, optical resolution 2 nm. T = 300 K, time 30 seconds. Spectrum performed, processed and interpreted by Antonello Dallegno.

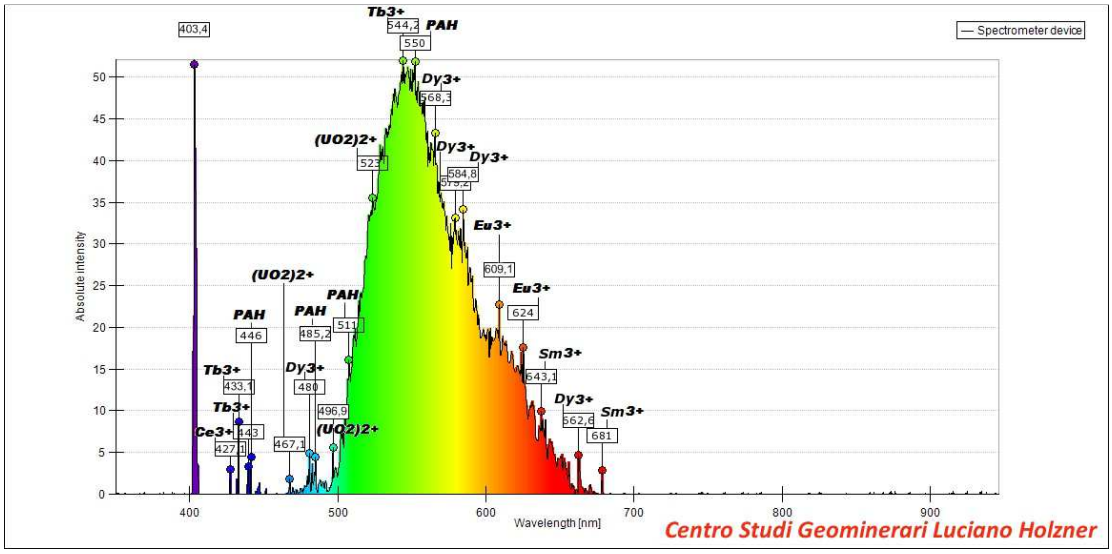

Drawing 4: Laser-induced steady-state luminescence spectrum of saccharoid, white to very pale gray quartz (sample CSG ls 33) showing $(UO_2)^{2+}$,Tb^{3+}, Ce^{3+}, PAHs, Eu^{3+}, Dy^{3+} and Sm^{3+} fluorescence centers. Note the clear extension towards yellow-orange-red regions of the spectrum, compared with the spectrum from white fibrous-radiating quartz (Drawing 2). This difference is due to a greater amount of Dy^{3+} and Sm^{3+} fluorescence centers. λex = laser diode 405 nm 500 mW, optical resolution 0,5 nm, T = 300 K, time 1 second. Spectra performed, processed and interpreted by Antonello Dallegno.

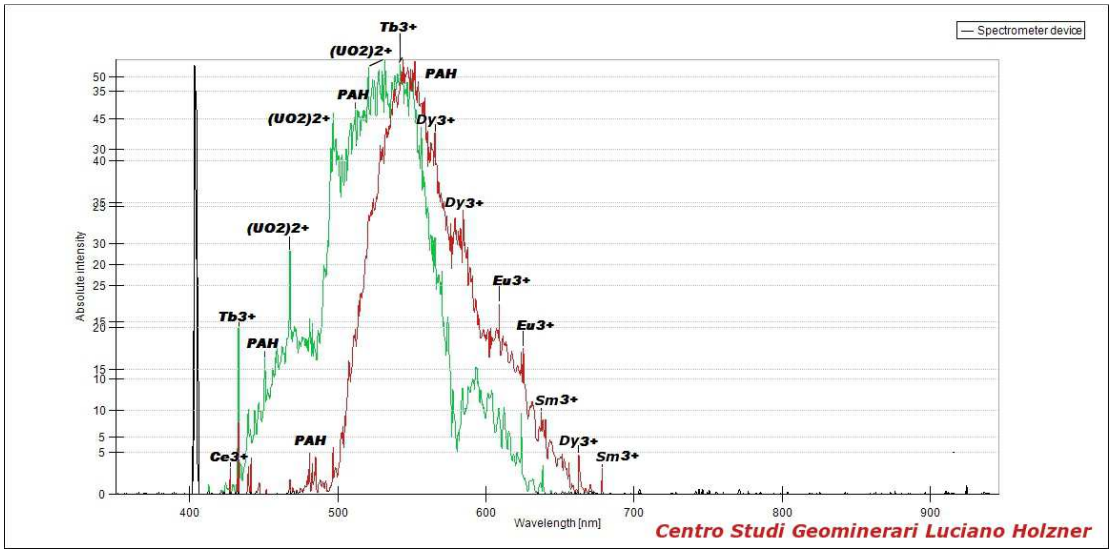

Drawing 5: Two overlapping laser-induced steady-state luminescence spectra. Green line: spectrum measured on the whitish fibrous radiating quartz (λex = laser diode 405 nm 500 mW, optical resolution 0,5 nm, T = 300 K, time 1 second. Red line: spectrum measured on the whitish saccharoid quartz (λex = laser diode 405 nm 500 mW, optical resolution 0,5 nm, T = 300 K, time 1 second. Saccharoid quartz spectrum is clearly shifted toward red, due to minor presence of $(UO_2)^{2+}$, combined with the presence of Dy^{3+} and minor Sm^{3+} fluorescence centers. Spectra performed, processed and interpreted by Antonello Dallegno.

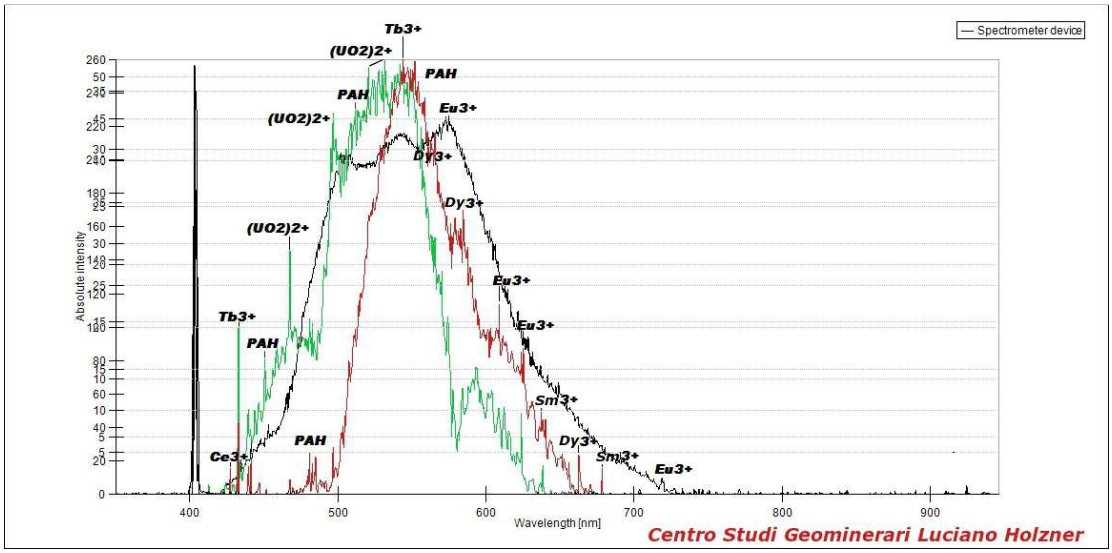

Drawing 6: Three overlapping laser-induced steady-state luminescence spectra. Green line: spectrum measured on the whitish fibrous radiating quartz; red line: spectrum measured on the whitish saccharoid quartz (λex = laser diode 405 nm 500 mW, optical resolution 0,5 nm, T = 300 K, time 1 second). Black line: spectrum measured on the euhedral 'artichoke-type' pale honey yellow quartz crystals (λex = laser diode 405 nm 300 mW, optical resolution 2 nm, T=300 K, time 30 seconds). Spectra performed, processed and interpreted by Antonello Dallegno.